Metastable polymorphs of hydrogen isotopes solidified near the triple point

B. J. Kozioziemski, A. A. Chernov, E. R. Mapoles, and J. D. Sater
Lawrence Livermore National Laboratory, 7000 East Avenue, Livermore, California 94551, USA
(Received 17 March 2010; published 30 July 2010)

Hydrogen (H_2), deuterium (D_2), and the 0.25D_2-0.5DT-0.25T_2 isotopic mixture of deuterium and tritium (D-T) each form a metastable solid state below their respective triple-point temperatures (T_{TP}). The metastable solid is observed to nucleate and grow from inside of a 5–10 μm inner diameter borosilicate glass tube when the liquid hydrogens are slowly cooled through their respective T_{TP}. These metastable solids have their triple-point temperature 15–43 mK below the stable hexagonal close-packed (hcp) crystal of the same composition, a different growth habit, and recrystallize to the hcp solid. This metastable solid may be a crystal with unknown structure or, less likely, hcp with stacking faults and other defects.

DOI: 10.1103/PhysRevB.82.012104 PACS number(s): 81.30.Hd, 64.70.dg, 67.80.−s

Hydrogen and its isotopes are known to crystallize in the hexagonal close-packed (hcp) structure when cooled from the liquid through the triple point.[1] However, other structures are found with other solidification conditions. The structure is face-centered cubic (fcc) when deposited at less than 4 K directly from the vapor, when the $J=1$ rotational population is high (due to orientational ordering of the molecules), or under pressure.[1] One study found that H_2 and D_2 would form an fcc structure when grown from the liquid on a cube-textured gold foil.[2] A mixture of hcp and fcc was observed when depositing $J=0$ D_2 and H_2 onto a MgF_2 substrate at temperatures of $0.2–0.3T_{TP}$, where T_{TP} is the triple-point temperature.[3] However, the fcc converted to hcp when the sample was warmed. Disordered solids have also been observed for gases condensed into confined geometries such as Vycor glass[4,5] and cylindrical pores.[6]

The rare gas solids (except He) form the fcc phase, although a metastable hcp phase was reported for polycrystalline argon.[7] Small clusters have been shown to form an icosahedral structure that transforms to fcc with increasing cluster size,[8,9] with stacking faults responsible for the transformation.[10,11] Prediction and control of polymorphs of simple Lennard-Jones crystals remains an active area of study.[12,13]

We have observed the hydrogen isotopes to solidify into a metastable solid state in our inertial confinement fusion (ICF) assemblies. There are four key observations that suggest a metastable solid. First, the triple-point temperature of the metastable solid is lower than the stable hcp solid by 40 mK, 22 mK, and 16–22 mK for H_2, D_2, and D-T respectively. The second observation is a sudden recrystallization that produces many visible grain boundaries and defects on time scales of 10 s to minutes. Third, nucleation and growth of the hcp solid occurs at the expense of the already present metastable solid. Finally, the crystallographic growth shape anisotropy typical of the hcp solid is missing in the metastable solid. A determination of the nature of the metastable solid has not yet been made. The likely candidates are that it is a hcp structure with defects, e.g., the hcp/fcc mixture full of stacking faults (SF) and twins, or more likely a regular polymorph with unknown structure consistent with the Ostwald rule of stages.[14] Our observations suggest that the micro-meter scale geometry of fill-tube geometry is responsible for initiating the metastable phase.

The ICF assembly consists of a 2 mm OD, 40–150 μm thick spherical ablator shell composed of either beryllium or plastic. A 5–10 μm diameter hole is laser drilled into the shell and a fill-tube is attached to first evacuate then admit the hydrogen gas sample to the shell.[15–17] Figure 1 shows the section of the shell and fill-tube. The fill-tube is made of borosilicate glass, with one end epoxied into the shell and the other into a larger diameter polyimide-coated fused-silica glass. The shell is suspended by polyimide films inside of a hollow 5.5 mm diameter, 10 mm long aluminum cylinder (hohlraum). The cylinder is mechanically and thermally connected to a cryostat and cooled to 14–20 K. The cylinder has four calibrated Cernox resistance thermometers and four wound heaters and is filled with 1 torr of helium gas to conductively cool the shell. The calibrations are only accurate to ± 50 mK and a temperature offset exists between the shell and the cylinder (due to, for example, beta-decay heating). Therefore, temperature measurements are reported relative to T_{TP}, determined by observing the crystal to be neither growing nor shrinking. Active control of the heater power, with the thermometers as input, allows T_{TP} to be found to ± 0.25 mK. The hydrogen gas is admitted to the shell where it condenses as liquid under its own vapor pressure. Characterization is performed using x-ray imaging along one axis,[18,19] and optical microscopy[20] along the perpendicular axis, both in the horizontal plane.

The metastable solid was first observed with the D-T mixture. The isotopic composition of the D-T mixture is nominally 25%D_2-50%DT-25%T_2, but is not measured at the time of use. The above experiments were repeated using D_2

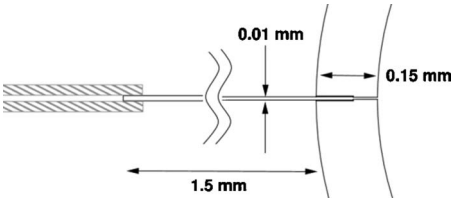

FIG. 1. Detail of the shell and fill-tube assembly showing the section of the spherical ablator shell 0.15 mm thick with the fill-tube. The borosilicate fill-tube is 0.010 mm in diameter where it enters the shell, tapering up to 0.020 mm where it is inserted into the larger diameter polyimide-coated silica-glass tube.

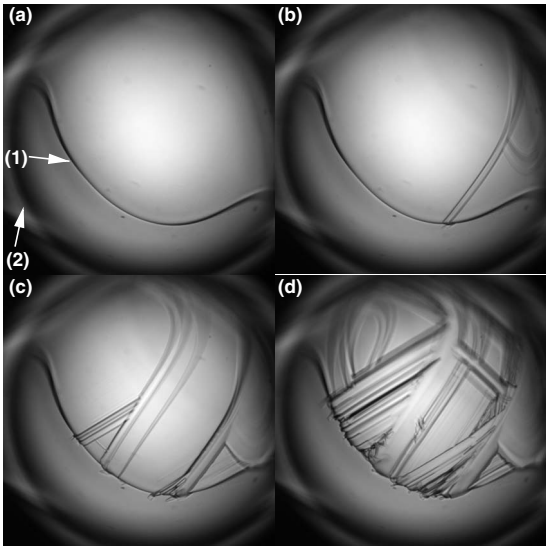

FIG. 2. Back-lit visible light images taken during recrystallization of D_2. The metastable solid is at the top of the images, with the arrow (1) in (a) pointing to the solid-vapor interface and arrow (2) pointing to the outer shell surface. The metastable solid was solidified from the liquid over 7 h at $T^*_{TP}-1.5$ mK, and is constant for the four images. Images are taken (b) 11 s, (c) 56 s, and (d) 120 s after (a) and show the conversion of the featureless metastable solid to the stable hcp solid. The observed features are grain boundaries separating the now polycrystalline hcp solid.

in the same shell that had previously been used with D-T. Finally, H_2 and D_2 where used in a new assembly prior to D-T. This excludes radiation damage from the tritium β-decay as the cause of the metastable phase. The H_2 and D_2 were research purity, 99.9999% and 99.5%, respectively, with 0.5% HD being the dominant impurity in the D_2 gas. The metastable solid was observed with both H_2 and D_2.

The metastable solid is formed as follows. Solid initially in the shell is melted by raising the temperature 2–50 mK above the hcp solid triple-point temperature, T^I_{TP}. Solidification inside the shell typically begins at the fill-tube and propagates into the shell when $T^I_{TP} > T > T^I_{TP}-50$ mK, with the undercooling decreasing with increasing isotope mass. In some cases, the hcp c-plane emerges typically parallel, but sometimes normal to the fill-tube axis.[21] However, the metastable solid can emerge from the fill-tube instead, appearing much more often within the 5–10 μm inner diameter (ID) borosilicate fill-tubes than the previous 30–40 μm fused silica (SiO_2) fill-tubes.

Figure 2 shows the optical microscope images of the D_2 metastable solid and its recrystallization. In these images gravity is down, the supporting polyimide films are visible out-of-focus at the top and bottom of the shell, and the fill-tube enters from the left side of the image at the center plane of the shell. The microscope is focused on the side of the shell closest to the camera. The temperature was held 1.5 mK below T^*_{TP} for 7 h. The metastable D_2 and H_2 solids needed to be held within 1.5 mK of T^*_{TP} until all the liquid solidified to prevent recrystallization. The 1×10^{-3} cc liquid, approximately 1/5 of the shell's inner volume, solidified in 4–5 h and the solid slowly migrated due to the vertical thermal

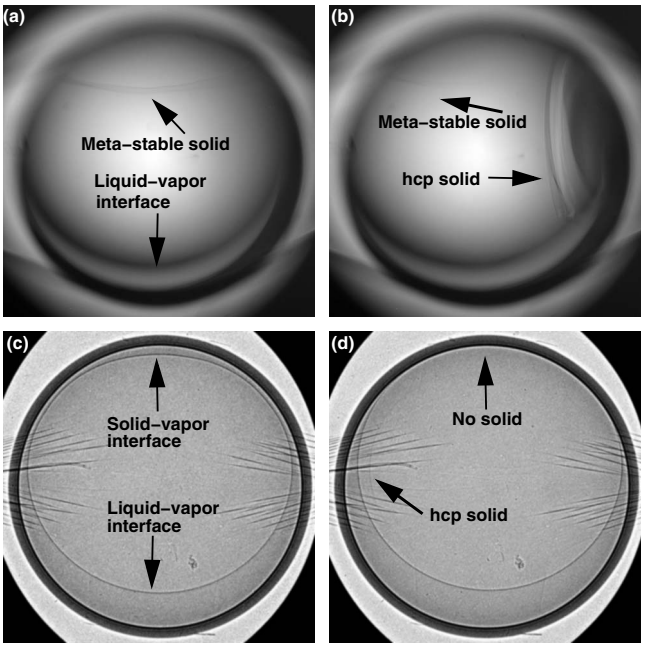

FIG. 3. Visible (top) and x-ray images (bottom) of D-T just before and after recrystallization. Image (a) is 34 s before the recrystallization event, (b) 26 s after. Image (c) is taken 10 s before recrystallization, (d) 120 s after recrystallization. In (a) and (c) the metastable solid is located at the top of the image, with the arrow in (a) pointing to the interface between the metastable solid and liquid. In (b), the hcp solid has nucleated and is growing on the right and the arrow points in the direction of the retreating metastable solid. (d) shows that the metastable solid at the top of (c) is gone within 120 s of the nucleation of the hcp solid. X-ray images are orthogonal to the visible images. The fill-tube enters from the left side in all images.

gradient over the next 2–3 h. The solid varies in thickness from 0 to 400 μm around the shell surface. Figure 2(a) is taken just before the recrystallization begins. The solid-vapor interface is indicated by the arrow (1), with the solid in the upper portion of the shell. Figures 2(b)–2(d) were taken with the temperature held constant at 11 s, 56 s, and 120 s after (a), respectively. Increasing numbers of grain boundary grooves, separating the new hcp grains along the intersection of grain boundaries with the crystal-vapor interface, replace the featureless solid of (a) as the recrystallization occurs. Few changes to the solid are visible after $\approx$600 s. The solid melts at T^I_{TP}, not T^*_{TP} after recrystallization.

Figure 3 shows visible (top) and x-ray (bottom) images just before and after the recrystallization of D-T from the metastable to stable solid. Panels (a) and (c) show the metastable solid near the top of the shell. As in Fig. 2, the metastable solid emerged from the fill-tube. The temperature was then increased by 3 mK and held constant to keep the solid volume approximately constant. The solid migrated from the center plane to the colder top of the shell. Panels (a) and (c) were taken about 1 h after the metastable solid emerged from the fill-tube. The x-ray image shows that the surface tension draws the liquid up the side of the shell into contact with the solid phase. It also shows that the metastable solid is up to 60 μm thick at the very top of the shell and 700–1000 μm

TABLE I. Triple-point temperature difference between metastable and hcp solids. $J=1$ concentrations estimated from known rates.

Isotope	$J=1$(%)	ΔT_{TP} (mK)
H_2	72–75	42.0 ± 2.0
H_2	32–38	37.5 ± 0.7
D_2	33	21.0 ± 1.0
D_2	12–18	22.2 ± 0.5
D-T	<2	16.5 ± 1.0
D-T	2–26	22.0 ± 1.0

in lateral extent. Panels (b) and (d) show the corresponding images just after recrystallization. The optical image shows the disappearance of the metastable solid at the top of the shell and the nucleation and growth of the stable hcp solid on the right side of the image. Panels (a) and (b) are 60 s apart. The x-ray image in panel (d) shows that the metastable solid is gone within 120 s of the start of recrystallization. The fill-tube, partially masked by straight lines of the support films, is visible in (c) and (d) entering from the left and stopping just short of the shell center.

Figures 2 and 3 show two examples where the metastable D_2 and D-T solids can be held neither growing nor shrinking 22 and 16.5 mK below T_{TP}^{I}, respectively. Increasing the temperature by 0.5 mK results in the metastable solid completely melting. In contrast, once the recrystallization event occurs it is necessary to raise the temperature to T_{TP}^{I} to completely melt the solid in the shell. Table I shows the difference between the hcp and metastable solid triple-point temperatures, ΔT_{TP}, for H_2, D_2, and D-T. The $J=1$ concentration is calculated based on the self-conversion rates[22] for the H_2 and D_2 samples, using the liquid and solid conversion times to set the range. Only a weak dependence of ΔT_{TP} is observed with the $J=1$ concentration.

The metastable solid was identified in a search of our previous experimental images for one shell with a 40 μm fill-tube suspended vertically in a spherical cavity. The metastable solid appeared with a frequency of less than 10% of the nucleation attempts for that shell. Additional experiments were carried out with H_2 and D_2 using an older style shell and fill-tube assembly, consisting of a 30–40 μm diameter fused-silica glass fill-tubes with plastic shells.[18,21,23–26] The metastable solid was not observed with the fill-tube either horizontal or vertical with the larger silica glass fill-tubes. Furthermore, the metastable solid appears in Be shells with the small-diameter fill-tubes, based on x-ray images and ΔT_{TP}.

We do not yet have diffraction data to characterize the structure of the metastable sold. Thus we will use the available data to analyze if the metastable solid is either a new hydrogen polymorph with unknown structure or a hcp solid containing many stacking faults (SF), twins, dislocations, and/or grain boundaries. The amorphous solid is not considered here because it exists at $T\lesssim 0.5T_{TP}$.[27]

The upper limit to the defect density may be estimated as follows. We assume the total energy of the defects is responsible for the difference of the chemical potential $\Delta\mu$ of the metastable solid over the hcp solid. This $\Delta\mu$ value determines the shifts ΔT and ΔP of the temperature and pressure of the triple-point between the metastable solid and the hcp solid (S) with the same liquid (L) and vapor (V),

$$\Delta T=(\omega_V-\omega_S)\Delta\mu/D,\quad \Delta P=(s_V-s_L)\Delta\mu/D,$$

$$D\equiv(s_V-s_S)(\omega_L-\omega_S)-(s_L-s_S)(\omega_V-\omega_S). \qquad (1)$$

Here ω and s are the molecular volumes and entropies of the phases indicated by the subscripts. For D-T, $\omega_V=1.33\times10^{-20}$ cm^3, $\omega_L=3.75\times10^{-23}$ cm^3, $\omega_S=3.30\times10^{-23}$ cm^3, $s_V-s_S=1.33\times10^{-15}$ erg/K, $s_L-s_S=1.83\times10^{-16}$ erg/K.[22] Then $\Delta\mu=3.01\times10^{-18}$ erg, $\Delta P=142$ Pa (compared to the D-T saturated vapor pressure of 20080 Pa).

The elastic strain that would raise the hcp chemical potential by $\Delta\mu$ is $\epsilon\approx(2\Delta\mu/E\omega_S)^{1/2}\approx6\times10^{-3}$, using the Young's modulus $E=5\times10^9$ erg/cm^3.[28] The residual strain storing the same energy $\Delta\mu$ would be generated by $\approx2\times10^{12}$ dislocations/cm^2, or by SF with the average distance of $\approx$200 lattice spacings in between. The former number comes from the assumption that the SF energy is proportional to the evaporation enthalpy over the area $\omega^{2/3}$ per one molecule at an interface. That scaling works for the measured SF energy[29] with the proportionality factor 7.2×10^{-3} and estimates the SF energy in D-T to be 0.18 erg/cm^2. Previously,[21] the difference in the D-T and shell thermal expansion coefficient led to the thermoplastic strain 2×10^{-3}, comparable with the above calculated strain of 6×10^{-3}. The thermoplastic strain relaxed, forming optically visible grain boundary grooves within one minute. On the contrary, the metastable solid remained homogeneous for up to 48 h of annealing near T_{TP}^{*}, and also down to 0.25 K below T_{TP}^{*}. This behavior makes it unlikely that the dislocation network is responsible for the metastable solid.

The SF are less mobile than dislocations so that the SF structures should be more stable to annealing. Formation of the SF may also lead to the hcp/fcc mixing.[30] However, no morphological features develop in the metastable solid neither during annealing nor when it migrates along the shell wall due to an applied thermal gradient. There is no crystallographic anisotropy on the smooth or wavy border of the metastable solid. That behavior excludes the reproduction of stacking fault sequence during growth by deposition of lattice layers generated by screw dislocations on a singular face, like in SiC growing layer by layer from the vapor. The lack of noticeable stress in hydrogens slowly growing near the melting temperature eliminates the similar replication of SFs in the material bulk by the Frank-Reed dislocation sources. Nearly parallel SFs crossing the growth front should merge with one another at the growth front, thus decreasing the SF density and ΔT_{TP}. However, experiments show no dependence of ΔT_{TP} on the growth rate or history in general. The SF and twin formation occurs at high supersaturations in small particles but not in large samples.[10] Table I shows that ΔT_{TP} decreases when the isotope mass increases. That sequence is opposite to the T_{TP} sequence, evaporation enthal-

pies, and thus SF energies. The same data in Table I above suggest a moderate effect of the $J=1$ concentration on the metastable solid.

The facts and arguments above suggest that the metastable solid is more likely a hydrogen polymorph rather than an hcp solid with defects. Determination of the solid structure of the polymorph requires diffraction studies. Here we may only speculate that the close packing requirement might result in fcc, icosahedrons, or even quasicrystalline features in the structure, as observed in models with Lennard-Jones systems.[12,13]

The metastable solid may be a surface induced phase. The nucleation requires supercooling of only 3–20 mK relative to T_{TP}^{*}, if initiated after melting the previous solid by T_{TP}^{I} $+(1-50)$ mK. The liquid often reaches supercoolings of 0.5–1.5 K before nucleation if the temperature is taken to $T_{TP}^{I}+(100-500)$ mK. This effect[30] suggests that nucleation occurs on the subsurface crystalline islands not completely disordered by melting. The borosilicate glass fill-tube with the $5-10$ μm ID most often generates the metastable solid. Although the $5-10$ μm ID is large compared to other confined geometries,[8] its geometry likely plays a role in formation of the metastable solid.

In summary, a metastable polymorph of solid H_2, D_2, and D-T in equilibrium with both vapor and liquid at 43–16 mK below the respective hcp T_{TP} has been observed. The solid does not change after annealing. When the regular hcp solid appears it grows at the expense of the metastable solid. The new solid has an isotropic growth rate; it may grow and recrystallize preserving its properties. The unknown solid might be either a real polymorph with unknown structure, or, less likely, an hcp/fcc mixture with high density of stacking faults and twins entangled with other defects.

Our gratitude goes to G. Gilmer for valuable discussions. This work was performed under the auspices of the U.S. Department of Energy by Lawrence Livermore National Laboratory under Contract DE-AC52-07NA27344.

[1] I. F. Silvera, Rev. Mod. Phys. **52**, 393 (1980).
[2] C. S. Barrett, L. Meyer, and J. Wasserman, J. Chem. Phys. **45**, 834 (1966).
[3] G. W. Collins, W. G. Unites, E. R. Mapoles, and T. P. Bernat, Phys. Rev. B **53**, 102 (1996).
[4] D. W. Brown, P. E. Sokol, and S. N. Ehrlich, Phys. Rev. Lett. **81**, 1019 (1998).
[5] Y. Wang, W. M. Snow, and P. E. Sokol, J. Low Temp. Phys. **101**, 929 (1995).
[6] K. Morishige and K. Kawano, J. Phys. Chem. B **104**, 2894 (2000).
[7] L. Meyer, C. S. Barrett, and P. Haasen, J. Chem. Phys. **40**, 2744 (1964).
[8] S. I. Kovalenko, D. D. Solnyshkin, E. A. Bondarenko, and E. T. Verkhovtseva, Low Temp. Phys. **23**, 140 (1997).
[9] S. I. Kovalenko, D. D. Solnyshkin, and E. T. Verkhovtseva, Low Temp. Phys. **26**, 207 (2000).
[10] S. I. Kovalenko, D. D. Solnyshkin, E. T. Verkhovtseva, and V. V. Eremeko, Chem. Phys. Lett. **250**, 309 (1996).
[11] S. I. Kovalenko, D. D. Solnyshkin, E. A. Bondarenko, E. T. Verkhovtseva, and V. V. Eremenko, J. Cryst. Growth **191**, 553 (1998).
[12] C. Desgranges and J. Delhommelle, Phys. Rev. Lett. **98**, 235502 (2007).
[13] N. L. Abraham and M. I. J. Probert, Phys. Rev. B **77**, 134117 (2008).
[14] W. Ostwald, Z. Physik. Chem. **22**, 289 (1897).
[15] S. W. Haan, T. Dittrich, G. Strobel, S. Hatchett, D. Hinkel, M. Marinak, D. Munro, O. Jones, S. Pollaine, and L. Suter, Fusion Sci. Technol. **41**, 164 (2002).
[16] M. Takagi, K. Saito, C. Frederick, A. Nikroo, and R. Cook, Fusion Sci. Technol. **51**, 638 (2007).
[17] Z. Z. Johal, J. W. Crippen, A. C. Forsman, E. H. Lundgren, K. A. Moreno, and A. Nikroo, Fusion Sci. Technol. **55**, 331 (2009).
[18] B. J. Kozioziemski, J. D. Sater, J. D. Moody, J. J. Sanchez, R. A. London, A. Barty, H. E. Martz, and D. S. Montgomery, J. Appl. Phys. **98**, 103105 (2005).
[19] D. S. Montgomery, A. Nobile, and P. J. Walsh, Rev. Sci. Instrum. **75**, 3986 (2004).
[20] J. A. Koch, T. P. Bernat, G. W. Collins, B. A. Hammel, B. J. Kozioziemski, A. J. MacKinnon, J. D. Sater, D. N. Bittner, and Y. Lee, Fusion Technol. **38**, 123 (2000).
[21] A. A. Chernov *et al.*, Appl. Phys. Lett. **94**, 064105 (2009).
[22] P. C. Souers, *Hydrogen Properties for Fusion Energy* (University of California, Berkeley, 1986).
[23] J. Sater, B. Kozioziemski, G. W. Collins, E. R. Mapoles, J. Pipes, J. Burmann, and T. P. Bernat, Fusion Technol. **35**, 229 (1999).
[24] D. N. Bittner, G. W. Collins, E. Monsler, and S. Letts, Fusion Technol. **35**, 244 (1999).
[25] D. N. Bittner, G. W. Collins, and J. D. Sater, Fusion Sci. Technol. **44**, 749 (2003).
[26] B. J. Kozioziemski, R. L. McEachern, R. A. London, and D. N. Bittner, Fusion Sci. Technol. **41**, 296 (2002).
[27] E. Koresheva, I. Osipov, T. Timasheva, and L. Yaguzinskiy, J. Phys. D **35**, 825 (2002).
[28] A. I. Prokhvatilov, *Plasticity and Elasticity of Cryocrystals* (Begell House Publishers Inc., New York; Wallingford, UK, 2001).
[29] L. E. Murr, *Interfacial Phenomena in Metals and Alloys* (Addison Wesley Publishing Co., London, 1975).
[30] A. A. Chernov, E. I. Givargizov, K. S. Bagdasarov, V. A. Kuznetsov, L. N. Demianets, and A. N. Lobachev, *Modern Crystallography III. Crystal Growth*, Springer Series Solid State Vol. 36 (Springer, Heidelberg, 1984).